Emergent Phases in Optical Lattice

Huiming Xu

Department of Physics

(Dated: Dec.12, 2009)

Abstract

Optical lattice formed by counter propagating laser beams provides us a new platform to study condensed matter physics. Cold atoms moving in an optical lattice could be described by Bose-Hubbard Model. By controlling laser intensity, we could change interaction and tunneling strength at will. Thus, different quantum phases could occur in optical lattice. In this review, I will give an overview of different phases (i.e. Superfluid, Mott Insulating) in optical lattice. I will focus on the phase diagram and the characteristics of different phases.

Introduction:
Due to ac stack effect, atoms moving in optical fields will experience a potential, and the strength of potential is dependent on the strength of the local optical field. Thus, a three-dimensional optical lattice potential could be formed by aligning three optical standing waves orthogonal to each other. In a typical experiment, each standing wave laser field is created by focusing a laser beam to a waist of about $100 \ \mu m$ at the position of the condensate. A second lens and a mirror are then used to reflect the laser beam back onto itself, creating an interference pattern of standing optical wave. When the field strength of the three standing waves is the same, the three-dimensional optical lattice potential has the simple form [1]:

$$V_0(x) = V_0(sin^2(kx) + sin^2(ky) + sin^2(ky))$$

with wave vector $k = 2\pi/\lambda$, λ is the wave length of the laser light, corresponding to a lattice period $a = \lambda/2$. V_0 is the maximum depth of the optical lattice potential, which is proportional to the laser light intensity and the polarity of atoms. This depth is conveniently measured in units of recoil energy $E_R = \hbar^2 k^2/2m$. In the low temperature limit, this optical lattice potential could be approximated by a harmonic potential with trapping frequency $\nu_R \approx (\hbar k^2/2\pi m)\sqrt{V_0/E_R}$.

When the pair interaction is not taken into account, the motion of atoms in periodic lattice potential is well described within the band theory. This consists of vibrational motion within an individual well and tunneling between neighboring wells. At low enough temperatures, atoms will Bose condense and the condensate will be in a Superfluid state, where wave function exhibits long range coherence. In reality, there are repulsive pair interactions between atoms, and this may change the properties of the system dramatically depending on the strength of interaction. When the pair interaction strength is small compared to the tunneling strength, the condensate will remain in the superfluid state. A delocalized wave function will minimize the energy of the system and atoms could hop around freely. However, in the case of strong repulsive interactions and commensurate filling (each site has the same number of atoms), atoms will not be able to hop around freely as before. There will be a large energy cost for an atom to hop from one site to another due to the strong repulsive interaction between atoms (see Figure 1). Thus, the condensate will be in a mott-insulating state characterized by the existence of a gap for particle-hole excitations and by the zero compressibility [2]. Thus, the competition between tunneling and repulsive interaction will result in different emergent quantum phases. Optical lattice is a great system to study such phenomenon, because the relative strength of tunneling and repulsive interaction could be tuned by changing the brightness of laser light. In fact, a superfluid to mott-insulting quantum phase transition has been realized experimentally in 2002 [3].
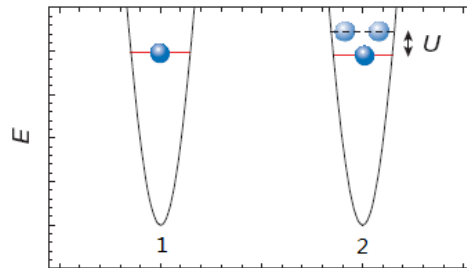
Figure 1: If the atom in site 1 hops to site 2, there will be an energy cost of U due to the repulsive interaction between two atoms in site 2 [3].

In this experiment, the superfluidity near the mott-insulating transition was inferred indirectly from coherence measurements. Since the observed excitation spectrum and atomic inference pattern did not change abruptly, the precise location of phase transition could not be determined. Later experiment extended the early work by studying stability of superfluid current as a function of momentum and lattice depth [5, 6]. The superfluid regime could be better characterized by observing a critical current for superfluid flow through the onset of dissipation. In this review, I will first introduce the Bose-Hubbard Model and the phase diagram of atoms in optical lattice. Then, the experiments on quantum phase transition from superfluid to mott-insulating will be introduced and compared.

Bose-Hubbard Model for atoms moving in optical lattice:
Cold atoms moving in periodic optical lattice potential could be described by Bose-Hubbard Model. The starting point is the Hamiltonian operator [1]

$$H = \int d^3 x \psi^\dagger(x) \left(-\frac{\hbar^2}{2m}\nabla^2 + V_0(x) + V_T(x) \right) \psi(x) + \frac{1}{2}\frac{4\pi a_s \hbar^2}{m} \int d^3 x \psi^\dagger(x)\psi^\dagger(x)\psi(x)\psi(x) \quad (1)$$

with $\psi(x)$ a boson field operator for atoms in a given internal atomic state, $V_0(x)$ is the optical lattice potential, and $V_T(x)$ is the slowly varying external harmonic tramping potential, e.g., a magnetic trap. In the low energy regime, the pair interaction between cold atoms could be described with a single s-wave scattering length a_s. This effective interaction is of contact type and isotropic with the form of $4\pi a_s \hbar^2/m$. The single particle wave function in a periodic potential is given by Bloch wave function, and a proper recombination of Bloch wave function would yield a set of well localized Wannier functions. In the cold atomic system, the energies involved in system dynamics are small compared to the excitation energies to the second band. So, we could assume there are no excitations to the second band. Thus we could expand our field operators in the set of Wannier functions formed only by first band Bloch wave functions. Then, field operator could be written as $\psi(x) = \sum_i b_i w(x - x_i)$. Substitute this into equation (1), we have the following Bose-Hubbard Hamiltonian

$$H = -J \sum_{<i,j>} b_i^\dagger b_j + \sum_i \epsilon_i n_i + \frac{1}{2}U \sum_i n_i (n_i - 1), \quad (2)$$

Where the operators $n_i = b_i^\dagger b_i$ count the number of bosonic atoms at site i; the annihilation and creation operators obey canonical commutation relations $[b_i, b_j] = \delta_{ij}$. The parameter $U = 4\pi a_s \hbar^2 \int d^3 x |w(x)|^4/m$ corresponds to the strength of the onsite repulsion of two atoms at site i. $J = \int d^3 x w^*(x - x_i) \left[-\frac{\hbar^2}{2m}\nabla^2 + V_0(x) \right] w(x - x_j)$ is the hopping matrix between two sites i and j. $< i, j >$ denotes the nearest neighbors. $\epsilon_i = \int d^3 x V_T(x)|w(x - x_i)|^2 \approx V_T(x_i)$ is the energy offset of each lattice site.

For a given optical potential, J and U could be evaluated numerically [1]. For the optical lattice potential given above, the Wannier function could be written as $w(x) = w(x)w(y)w(z)$ which can be determined from band structure calculations. Figure 2 shows J and U as a function of the parameter V_0 in units of recoil energy $E_R = \hbar^2 k^2/2m$. A larger lattice depth will lead to smaller tunneling J because of the higher energy barrier between neighboring sites. On the other hand, the atomic wave function will be more localized, and this leads to a stronger onsite repulsive pair

interaction U.
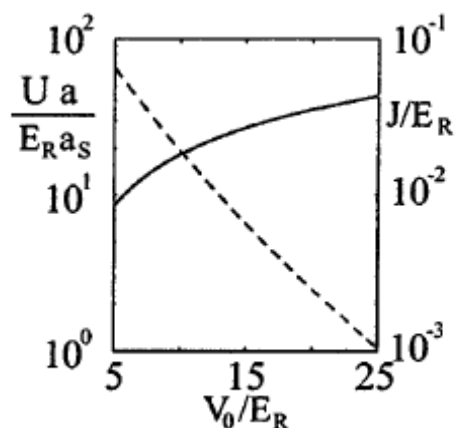
Figure 2: Plot of the scaled on site interaction U/E_R multiplied by a/a_s ($>>1$) (Solid line: axis on left-hand side of graph) and J/E_R (dashed line; axis on right-hand side of graph) as a function of V_0/E_R [1].

From Figure 2, we can see that by varying the optical lattice potential depth, a broad range of values of J and U could be reached. As a result, different quantum phases will show up if we vary the strength of optical lattice potential V_0.

Zero temperature phase diagram for cold atoms moving in optical lattice:
A qualitative analysis of the zero temperature quantum phase diagram of the Bose-Hubbard model was given in [2]. First, we study the homogenous case $(V_T(\mathbf{x}) = 0)$ where the energy offset of each site ϵ_i is zero. In grand canonical ensemble, the zero temperature phase diagram is determined by the minimization of $H' = H - \mu N$. N is the total number of atoms in the system, $N = \sum_i n_i$. In Figure 3, we show the phase diagram in $\mu - J$ plane.
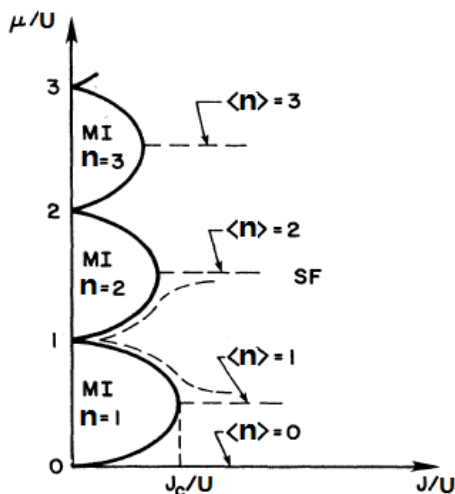
Figure 3: Zero temperature phase diagram of bosons in optical lattice. n is the average number of bosons per lattice site [2].

In the limit J = 0, each site i is occupied by n_i bosons which minimizes the on-site energy:

$$H_i'(n_i) = -\mu n_i + \frac{1}{2} U n_i (n_i - 1). \tag{3}$$

Since n_i must be an integer, when $n - 1 < \mu/U < n$, $n_i = n$ will minimize the onsite energy $H_i'(n_i)$. So, exactly n bosons will occupy each site when $n - 1 < \mu/U < n$. The system is in commensurate filling state, i.e. each site has the same number of particles. Now, fixing μ at a given value corresponding to n bosons per lattice site, i.e., $\frac{\mu}{U} = n - \frac{1}{2} + \alpha$, for some α in the range $-\frac{1}{2} < \alpha < \frac{1}{2}$, we turn on some weak hopping $J/U > 0$. The potential energy cost of adding or removing one particle to site i are given respectively by $\delta E_p = H_i'(n+1) - H_i'(n) = \left(\frac{1}{2} - \alpha\right) U$ and $\delta E_h = H_i'(n-1) - H_i'(n) = \left(\frac{1}{2} + \alpha\right) U$. So, when J is smaller than both δE_p and δE_h, the kinetic energy gained by adding (removing) a particle from the system and allowing the extra particle (hole) to hop around the lattice is insufficient to overcome the potential energy cost. As a result, for every positive n, there exists a finite region in the $\mu - J$ plane (Figure 3) in which the number of particles is fixed at precisely n per site. Moreover, in each such region, allowing one particle to hop from one site to the next gains roughly J in the kinetic energy at the expense of $\delta E_{ph} = \delta E_p + \delta E_h$ in potential energy. Because $J < \delta E_{ph}$, such hops are energetically costly. So, particles could not hop freely from one site to another when J is small compared to U. Thus, the regions of fixed n in Figure 3 represent mott-insulating phase with commensurate filling at each site.

The mott insulating phase is characterized by the existence of an energy gap, E_g, for the creation of particle or hole excitations, i.e. for the addition of particle to or, removal of particle from the system. For any point within the mott insulating phase in Figure 3, the gap E_g for particle (hole) excitation, is the distance in μ direction with J fixed from the upper (lower) phase boundary. In each Mott insulator phase, the lowest-lying excitation that conserves the total particle number is a particle plus hole excitation corresponds to the particle hopping from one site to the next site. The total energy cost of this excitation is the sum of particle and hole excitations which is the distance between upper and lower phase boundary in μ direction with J fixed. So, for a given J, the energy of this excitation is independent of μ.

The fact that the mott insulating phases have lobe-like shapes in Figure 3 could be understood as follows. If we start at a point within the mott insulating region, and increase μ at fixed J, eventually, we will reach a point where the potential energy cost of adding one particle to the system will be less than the kinetic energy gain of allowing it to hop around. In this case, it will be energetically favorable to add a particle to the system and let it hop around. Since, any non-zero density of particles free to hop around will Bose condense, producing a superfluid state in zero temperature, this point of energy balance defines the phase boundary for a transition between the mott insulating and superfluid state. Similarly, when we decrease μ with J fixed, eventually we will reach a point where the potential energy cost of removing a particle from the system is less than the kinetic gain of letting the created hole to hop around. In zero-temperature, any non-zero density of hole will also Bose condense and create superfluid state. As a result, whether we increase or decrease μ, we will eventually reach the phase boundary between mott insulating and superfluid state. Since the kinetic energy of mobile particles or holes is proportional to J, when we increase J, the width in μ of the mott insultating state will decrease.

Thus the mott insulating phases have lobe-like shapes in Figure 3. This concludes the qualitative analysis of the phase diagram in the homogeneous case.

In the above analysis, we only considered the homogeneous case, where the trapping potential $V_T(\mathbf{x}) = 0$. In real experiments, the trapping potential is not zero, but our above analysis will still work if we replace the chemical potential μ by its local counterpart $\mu - V_T(\mathbf{x})$. This is called the local density approximation and works well when $V_T(\mathbf{x})$ varies smoothly in space. Now, different lattice sites correspond to different local chemical potential. This may lead to a coexistence of superfluid and mott-insulating phases in the arrangement of a wedding cake in real space (see Figure 4a).
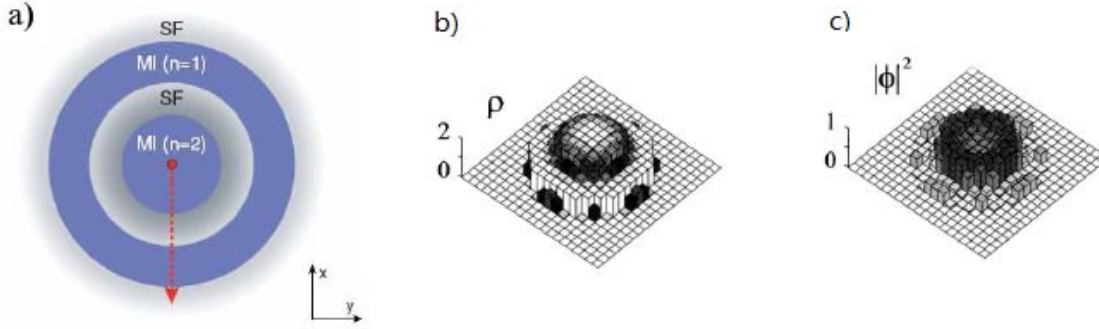
Figure 4: a) wedding cake structure of superfluid and mott-insulating phases; b) the density of cold atoms; c) the superfluid component. Parameters: $U = 35J$, $V_T(x,y) = J(x^2+y^2)/a^2$, and $\mu = 50J$ [1].

Aside from qualitative analysis, the detailed configuration of atoms moving in optical lattice could be calculated numerically using mean field theory [1]. The mean field calculations are based on a Gutzwiller ansatz for the ground state wave function $|\Psi_{MF}\rangle = \prod_i |\phi_i\rangle$ with $|\phi_i\rangle = \sum_{n=0}^{\infty} f_n^{(i)} |n\rangle_i$, where $|n\rangle_i$ denotes the Fock state with n atoms at site i. The coefficients $f_n^{(i)}$ are determined through the minimization of the expectation value of the Hamiltonian $\langle \Psi_{MF}|H - \mu N|\Psi_{MF}\rangle$ .Figure 4b,c show the density $\rho(x,y)$ and the superfluid component $|\phi(x,y)|^2$ in an optical lattice with a superimposed isotropic harmonic trapping potential in two dimensions. From Figure 4b,c, we can see there is a mott-insulating phase with two atoms per site at the center of the trap ($\rho = 2$) surrounded by a mott phase with a single atom ($\rho = 1$) and superfluid rings between the mott-insulating phases. For smaller values of the chemical potential, only a single mott phase would exist at the trap center.

Quantum phase transition from superfluid to mott insulating state:
In the above, we have derived the phase diagram of the cold atomic system in an optical lattice. Experimentally, it has been shown that by changing the depth of optical lattice potential, a quantum phase transition from superfluid to mott-insulating state could be realized. When optical lattice potential depth is small, the Bose-Einstein condensate is a superfluid and could be described by a wave function that exhibits long range phase coherence. If we suddenly turn off all the confining potential, the atomic gas wave function will expand and interfere with each other. Because of the long range coherence, the resulting absorption image of the atomic gas will have a high contrast interference pattern. However, if the optical lattice potential depth is large, the system would enter into the mott-insulating state and long range phase coherence no longer

exists. Thus, if we let the atomic gas expand freely, the absorption image will not show inference pattern as before. The detailed the experimental procedure is as below [3].

First, ^{87}Rb Bose-Einstein condensates are created and trapped magnetically. Then the trapped condensate is transferred into the optical lattice by slowly increasing the intensity of lattice laser beams to their final value over a period of 80 ms using an exponential ramp with a time constant of $\tau = 20ms$. The slow ramp speed ensures that the condensate always remains in the many body ground state of the combined magnetic and optical trapping potential. After raising the lattice potential the condensate has been distributed over more than 150,000 lattice sites with an average 2.5 atoms per lattice site in the center. In order to test whether there is still phase coherence between different lattice sites after ramping up the lattice potential, the combined trapping potential was suddenly turned off. The atomic wave functions are then allowed to expand freely and interfere with each other. In the superfluid regime, where all atoms are delocalized over the entire lattice with equal relative phases between different lattice sites, a high-contrast three-dimensional interference pattern as expected for a periodic array of phase coherent matter wave sources was observed (see Figure 5).
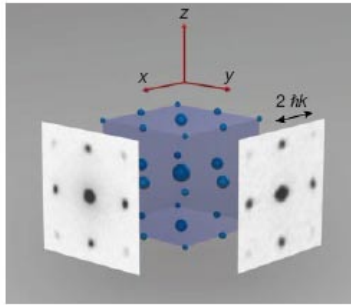
Figure 5: Schematic three-dimensional interference pattern with measured absorption images taken along two orthogonal directions. The absorption images were obtained after ballistic expansion from a lattice with a potential depth of $V_0 = 10E_R$ and a time of flight 15ms [3].

When the lattice potential depth is increased, the resulting interference pattern changes markedly (see Figure 6). Initially the strength of higher-order interference maxima increases as the potential height is raised, due to the tighter localization of the atomic wave functions at a single lattice site. Quite unexpectedly, however, at a potential depth of around $13E_R$, the interference maxima no longer increase in strength (see Figure. 6e). Instead, an incoherent background of atoms gains more and more strength until at a potential depth of $22E_R$ no interference pattern is visible at all. At this lattice potential depth, phase coherence has been completely lost. From Figure 6, we also see that during the evolution from the coherent to the incoherent state, there is no broadening of the interference peaks when the interference pattern is still visible. This behavior can be explained on the basis of the phase diagram. After the system has crossed the quantum critical point U/J=z*5.8, it will evolve in the inhomogeneous case into alternating regions of incoherent mott insulating phases and coherent superfluid phases where the superfluid fraction continuously decreases for increasing ratios U/J.
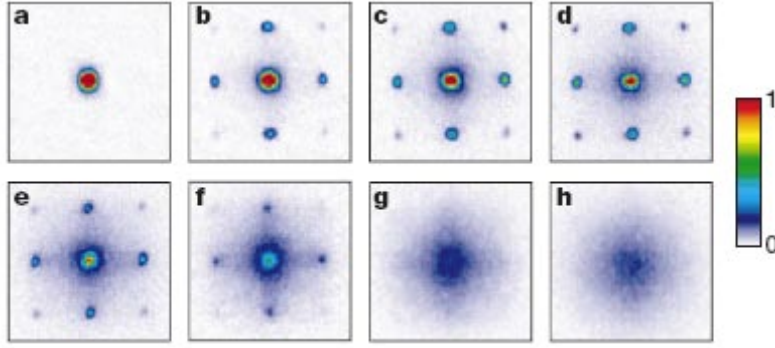
Figure 6: Absorption images of multiple matter wave interference patterns. These were obtained after suddenly releasing the atoms from an optical lattice potential with different potential depths V_0 after a time of flight 15ms. Values of V_0 were: a, $0E_R$; b, $3E_R$; c, $7E_R$; d, $10E_R$; e, $13E_R$; f, $14E_R$; g, $16E_R$; h, $20E_R$; [3]

Restoration of phase coherence:

A notable feature of mott-insulating state is that phase coherence could be rapidly restored if the optical lattice potential is lowered again to a value where the ground state of the condensate is completely superfluid [3]. It is shown in Figure 7b, that after only 4ms of ramp-down time, the interference pattern is fully visible again, and after 14ms of ramp-down time the interference peak has narrowed down to their steady-state value, proving that phase coherence has been restored over the entire lattice. It is interesting to compare this to that of a phase incoherent state, where random phases are present between neighboring sites. In phase incoherent state, there is no interference pattern even if the optical lattice potential has been ramped down (see Figure 7b).
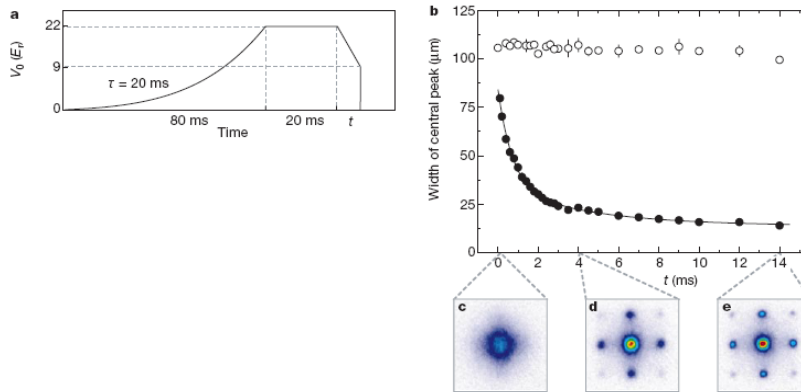
Figure 7: Restoring coherence. a, Experimental sequence used to measure the restoration of coherence after bringing the system into the mott insulating phase with $V_0 = 22E_R$ and lowering the potential afterwards to $V_0 = 9E_R$, where the system is superfluid again. The atoms are first held at the maximum potential depth V_0 for 20ms, and then the lattice potential is decreased to a potential depth of $9E_r$ in a time t after which the interference pattern of the atoms is measured by suddenly releasing them from the trapping potential. b, Width of the central interference peak for different ramp-down times t. In case of a mott-insulating state (filled circles) coherence is rapidly restored already after 4ms. For a phase incoherence state (open circles) using the same experimental sequence, no interference pattern reappears again, even for ramp-down times t of upto 400ms. The phase incoherent states are formed by applying a magnetic field gradient over a time of 10ms during the ramp-up period, when the system is still superfluid. c-e, Absorption images of the interference patterns coming from a mott-insulating state after ramp-down times t of 0.1ms (c), 4ms (d), 14ms (e) [3].

Excitation spectrum of mott-insulating phase:

Besides the loss of interference pattern, the mott-insulating state is also characterized by an energy gap in the excitation spectrum due to the repulsive onsite interaction. In the limit J<<U, the energy gap is U, which is the distance in μ direction between the upper and lower boundary of the mott lobe as mentioned before. Because of the energy gap, hopping of particles through the lattice is suppressed in the mott-insulating state. But, if the lattice potential is titled by the application of a potential gradient, tunneling is allowed again if the energy difference between neighbor sites equals the onsite interaction energy (see Figure 8).
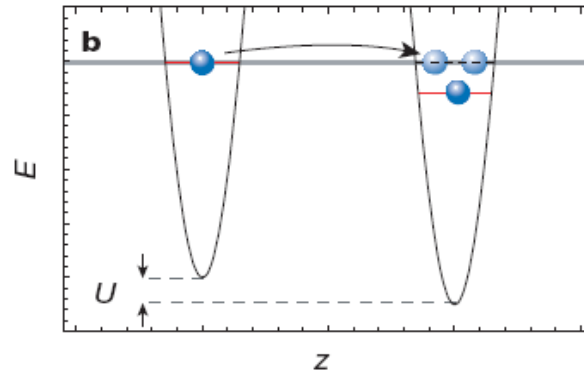
Figure 8: If a potential gradient is applied to the system along the z-direction, such that the energy difference between neighboring lattice sites equals the onsite interaction energy U, atoms are allowed to tunnel again. Particle-hole excitations are then created in the mott-insulating state [3].

The experimental procedure is shown in Figure 9a. It has been found that if excitations have been created during the application of the potential gradient at the potential depth $V_0 = V_{max}$, the condensate will not be able to return to the coherent superfluid state by subsequently lowering the potential depth again. Instead, excitations in the mott-insulating state will lead to excitations in the lowest energy band in the superfluid case. These excitations are simply phase fluctuations between lattice sites, and cause a broadening of the interference maxima in the interference pattern (see Figure 9b). Figure 9c-f shows the width of the interference peak versus the applied gradient potential [3].
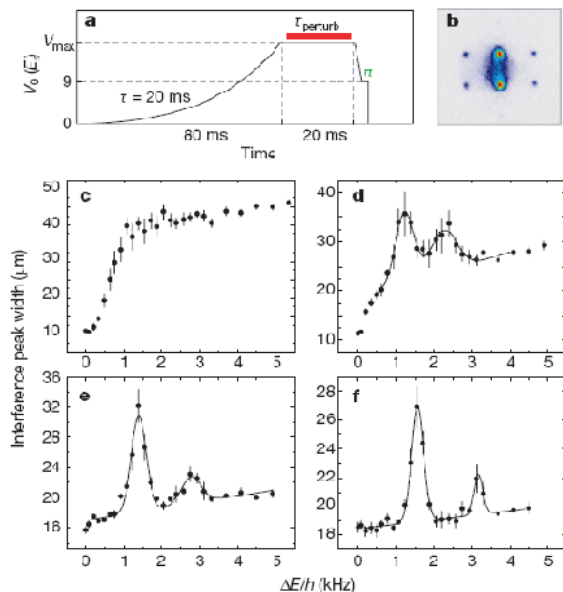
Figure 9 Probing the excitation probability versus an applied vertical potential gradient. **a**, Experimental sequence. The optical lattice potential is increased in 80 ms to a potential depth $V_0 = V_{max}$. Then the atoms are held for a time of 20 ms at this potential depth, during which a potential gradient is applied for a time $\tau_{perturb}$. The optical potential is then lowered again within 3 ms to a value of $V_0 = 9E_r$, for which the system is superfluid again. Finally, a potential gradient is applied for 300 μs with a fixed strength, such that the phases between neighbouring lattice sites in the vertical direction differ by π. The confining potential is then rapidly turned off and the resulting interference pattern is imaged after a time of flight of 15 ms (**b**). Excitations created by the potential gradient at a lattice depth of $V_0 = V_{max}$ will lead to excitations in the superfluid state at $V_0 = 9E_r$. Here excitations correspond to phase fluctuations across the lattice, which will influence the width of the observed interference peaks. **c–f**, Width of interference peaks versus the energy difference between neighbouring lattice sites ΔE, due to the potential gradient applied for a time $\tau_{perturb}$. **c**, $V_{max} = 10E_r$, $\tau_{perturb} = 2$ ms; **d**, $V_{max} = 13E_r$, $\tau_{perturb} = 6$ ms; **e**, $V_{max} = 16E_r$, $\tau_{perturb} = 10$ ms; and **f**, $V_{max} = 20E_r$, $\tau_{perturb} = 20$ ms. The perturbation times $\tau_{perturb}$ have been prolonged for deeper lattice potentials in order to account for the increasing tunnelling times. The solid lines are fits to the data based on two gaussians on top of a linear background.

From Figure 9, we can see that for a superfluid system at $10E_r$, the system is easily perturbed already for small potential gradients and for stronger gradients, a complete dephasing of wave functions leads to a saturation in the width of the interference peaks. At a potential depth of about $13E_r$, two broad resonances start to appear in the excitation spectrum, and for a potential depth of $20E_r$, a dramatic change in the excitation spectrum has taken place. The first resonance can be directly attributed to the creation of single particle-hole excitations in the mott-insulating state. The second resonance occurs at exactly twice the energy difference of the first, and can be attributed to one of the following processes: (1) simultaneous tunneling of two particles in a mott-insulating phase with $n > 1$ atoms, (2) second order processes, in which two particle-hole pairs are created simultaneously, with only one in the direction of the applied gradient, and (3) tunneling processes occurring between lattice sites with $n = 1$ atom next to lattice sites with $n = 2$ atoms. From the disappearance of interference pattern and the appearance of resonances in the excitation spectrum, the critical point of superfluid to mott-insulting phase transition could be determined. The critical lattice potential depth V_0 is between $10E_r$ and $13E_r$ [3]. This uncertainty is related to the inhomogeneous density profile of the trapped atoms and the fact that the interference pattern extends beyond the transition point due to short-range coherence in the mott-insulating phase [7]. Thus, the occurrence of peaks in the interference pattern is not a very precise indication of superfluidity [4].

Transport measurement of cold atoms in optical lattice:
Fortunately, besides phase coherence of wave function, the existence of a critical velocity is another characteristic feature of superfluidity. In the superfluid phase, current flows without dissipation if momentum does not exceed a critical momentum, while in the mott-insulating phase the critical momentum vanishes and transport is dissipative [5]. Thus, a transport measurement would better characterize the superfluid state by observing a critical current for superfluid flow and provide a clear distinction between the two quantum phases.

The experiment was done in the following way [5]. First, Bose-Einstein condensates were created and confined in an optical lattice. Then a moving lattice with velocity $v = \lambda \delta f / 2$ was created by introducing a small frequency detuning δf between the two counter propagating laser beams. If the velocity $v(t)$ changes slowly enough not to induce inter-band excitations, the initial Bloch state $|p = 0\rangle$ of the condensate in the optical lattice adiabatically evolves into the current carrying state $|p(t) = -mv(t)\rangle$ where p is the quasi-momentum. In a deep lattice potential, atoms will be dragged along with the moving lattice. Since the size of the trap is finite, atoms would reach the trap boundary in a short time. The problem was solved by first ramping up the lattice with $v = 0$, and then alternating the velocity of the moving lattice, thus performing a low-frequency ac transport measurement instead of dc. In a typical measurement, a sinusoidal momentum modulation of the moving lattice with amplitude p_M and period 10ms was applied. Then, the combined trapping potentials were turned off suddenly. After 33ms of ballistic expansion, the condensate fraction of the center peak of the superfluid interference pattern was recorded as a function of the momentum modulation amplitude p_M. To obtain a high contrast between the stable and dissipative regimes, several cycles of momentum modulation were applied. Figure 10a shows how the transition between superfluid and dissipative currents became sharper with increasing number of cycles of the momentum modulation. The critical momentum was determined from a log-log plot of the condensate fraction as a function of momentum p (see Figure 10c).

(a)

(b)

0 p_r   0.12 p_r   0.31 p_r   0.32 p_r   0.43 p_r
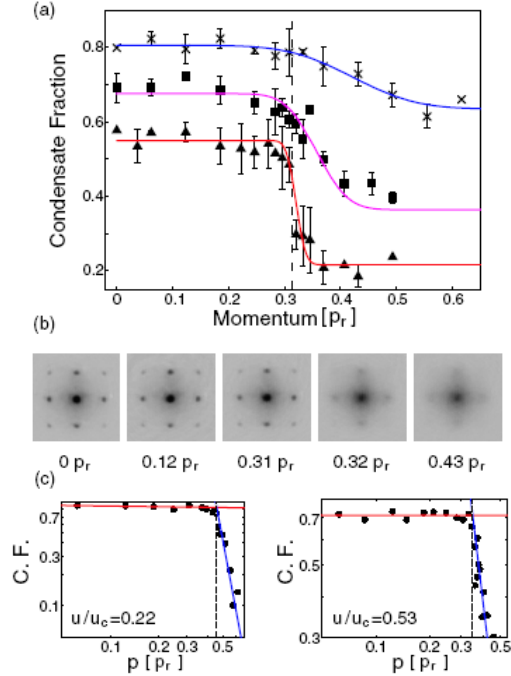
(c)

u/u_c=0.22

u/u_c=0.53

FIG.10 (color online). Determination of the critical momentum of superfluid flow. Shown is the condensate fraction as a function of a momentum p. (a) Condensate fraction with $u/u_c = 0.61$ for a variable number of cycles of the momentum modulation (one cycle: × and blue line, two cycles: ■ and purple line, three cycles: ▲ and red line). A dashed vertical line indicates the critical momentum where instability begins to occur. The two and three-cycle data are offset vertically for clarity. These data were fitted with an error function to guide the eye. (b) Images of interference patterns released from an optical lattice at $u/u_c = 0.61$ moving with variable momentum. Instability occurred between $p = 0.31 p_r$ and $0.32 p_r$. Some of the triangular data points in (a) were obtained from these images. (c) Condensate fraction on a log-log scale for two different interaction strengths.

The critical lattice depth for the superfluid to mott-insulating phase transition could be determined as the point where the critical momentum vanishes. Figure 11 shows the critical momentum versus the interaction strength u, where $u = U/J$. Theoretically, the critical momentum p_c near transition point has the following form: $p_c \propto \sqrt{1 - u/u_c}$ [6]. Using this form, the critical value $u_c = 34.2$ (± 2.0) has been determined. This corresponds to a lattice depth of 13.5 (± 0.2)E_r. Thus, the transport measurement can provide a better estimation of the critical point of the phase transition.
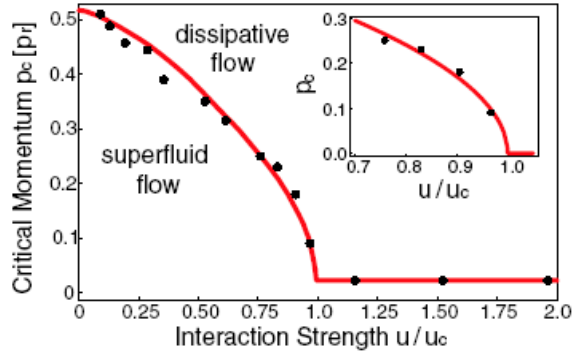
Figure 11: Critical momentum for a condensate in a 3D lattice. The solid line shows the theoretical prediction for the superfluid region. The horizontal solid line is a fit to the data points in the mott-insulating phase. (Inset) Fit of critical momentum near the superfluid to mott-insulating transition [6].

Conclusion:
In this essay, we studied the phase diagram of cold atomic system in optical lattice potential which could be described by Bose-Hubbard Model. We showed that depending on the relative strength of onsite interaction and U and tunneling J, the system could be in either superfluid or mott-insulting state. Experimentally, superfluid state is characterized by a distinct interference pattern, and mott-insulating state is characterized by a gap in the excitation spectrum. We also

showed that transport measurement revealed a critical momentum for superfluid flow. The existence of a critical momentum is a better indication of superfluid state. So, transport measurement can better locate the critical point for phase transition.

Reference:

1. Jaksch, D., Bruder, C., Cirac, J. I., Gardiner, C. W. & Zoller, P. Cold bosonic atoms in optical lattices. Phys. Rev. Lett. 81, 3108-3111 (1998).
2. Fisher, M. P. A.,Weichman, P. B., Grinstein, G. & Fisher, D. S. Boson localization and the superfluid insulator transition. Phys. Rev. B 40, 546-570 (1989).
3. Greiner, M., Mandel, O., Esslinger, T., Hansch, T., Bloch, I. Quantum phase transition from a superfluid to a Mott insulator in a gas of Ultracold atoms. Science 415, 39-44 (2002).
4. Diener, R., Zhou, Q., Zhai, H., Ho, T. Criterion for Bosonic Superfluidity in an Optical Lattice. Phys. Rev. Lett. 98, 180404 (2007).
5. Mun, J., Medley, P., Campell, G., Marcassa, L., Pritchard, D., Ketterle, W. Phase Diagram for a Bose-Einstein Condensate Moving in an Optical Lattice. Phys. Rev. Lett. 99, 150604 (2007).
6. Altman, E., Polkovnikov, A., Demler, E., Halperin, B., and Lukin, M. Superfluid-Insulator Transition in a Moving System of Interacting Bosons. Phys. Rev. Lett. 95, 020402 (2005).
7. Gerbier, F., Widera, A., Folling, S., Mandel, O., Gericke, T., Bloch, I. Phase Coherence of an Atomic Mott Insulator. Phys. Rev. Lett. 95, 050404 (2005).